INTERNATIONAL JOURNAL FOR NUMERICAL METHODS IN FLUIDS, VOL. 22, 673–688 (1996)

AN APPROXIMATE PROJECTION SCHEME FOR INCOMPRESSIBLE FLOW USING SPECTRAL ELEMENTS

L. J. P. TIMMERMANS, P. D. MINEV AND F. N. VAN DE VOSSE

Department of Mechanical Engineering, Eindhoven University of Technology, PO Box 513, NL-5600 MB Eindhoven, The Netherlands

SUMMARY

An approximate projection scheme based on the pressure correction method is proposed to solve the Navier–Stokes equations for incompressible flow. The algorithm is applied to the continuous equations; however, there are no problems concerning the choice of boundary conditions of the pressure step. The resulting velocity and pressure are consistent with the original system. For the spatial discretization a high-order spectral element method is chosen. The high-order accuracy allows the use of a diagonal mass matrix, resulting in a very efficient algorithm. The properties of the scheme are extensively tested by means of an analytical test example. The scheme is further validated by simulating the laminar flow over a backward-facing step.

KEY WORDS: Navier–Stokes equations; projection methods; operator splitting; spectral element methods

1. INTRODUCTION

The solution of the Navier–Stokes equations for unsteady incompressible fluid flow is still a major challenge in the field of computational fluid dynamics. An overview of the most important aspects with respect to the solution of the incompressible Navier–Stokes equations can be found in References 1–5. The Navier–Stokes equations form a set of coupled equations for both velocity and pressure (or, better, the gradient of the pressure). One of the main problems related to the numerical solution of these equations is the imposition of the incompressibility constraint and consequently the calculation of the pressure. The pressure is not a thermodynamic variable, as there is no equation of state for an incompressible fluid. It is an implicit variable which instantaneously 'adjusts itself' in such a way that the velocity remains divergence-free. The gradient of the pressure, on the other hand, is a relevant physical quantity: a force per unit volume. The mathematical importance of the pressure in an incompressible flow lies in the theory of saddle-point problems (of which the steady Stokes equations are an example), where it acts as a Lagrangian multiplier that constrains the velocity to remain divergence-free.[1,4]

There are numerous approaches to solve the Navier–Stokes equations. For the solution of unsteady Navier–Stokes flow perhaps one of the most successful approaches to date is provided by the class of projection methods.[6–8] Projection methods have been developed as a useful way of obtaining an efficient solution algorithm for unsteady incompressible flow. In this paper, projection methods are considered that are applied to the set of continuous equations, yielding very efficient and simple-to-implement algorithms. By decoupling the treatment of velocity and pressure terms, a set of easier-to-solve equations arises: a convection–diffusion problem for the velocity, yielding an intermediate velocity which is not divergence-free; and a Poisson equation for the pressure (or a related quantity).

CCC 0271–2091/96/070673–16

Received 19 May 1994
Revised 17 May 1995

There are essentially two approaches for continuous projection methods: fractional step methods and pressure correction methods.

The fractional step method[9–11] is based on a full splitting of the treatment of the pressure/incompressibility constraint and the diffusion in different substeps. The intermediate step leads to a Poisson equation for the pressure at the new time level. While the pressure is well-defined up to an arbitrary constant by the original equations, it is less so when directly expressed in terms of a Poisson equation. This is because in the latter case the necessity arises to formulate a non-trivial boundary condition for the pressure. The choice of the pressure boundary condition is an aspect that is much discussed in the literature.[9,12,13] The obvious theoretical choice for the pressure boundary condition is a Neumann condition derived from the normal component of the momentum equation. The form in which this boundary condition is implemented is important not only because of the overall accuracy but also because of the efficiency of the numerical scheme. This aspect is still very much open for improvement.

Pressure correction methods[14,15] consist of a basic predictor–corrector procedure between the velocity and pressure fields. Using an initial approximation of the pressure, the momentum equation can be solved to obtain an intermediate velocity field. This velocity in general does not satisfy the divergence-free constraint and must therefore be corrected. By taking the divergence of the momentum equation and enforcing the incompressibility constraint, a Poisson equation for the pressure correction (the difference between the new and the old pressure) is obtained. Using the pressure correction, the new velocity field can then be computed. An advantage of the pressure correction technique is that, contrary to the full splitting approach, the final velocity is guaranteed to satisfy the incompressibility constraint; of course, this is only true for the velocity in the continuous (semidiscrete) formulation. A drawback of this continuous approach is that in order to ensure divergence freedom, a homogeneous Neumann condition for the Poisson equation for the pressure correction must be used, which clearly is not valid for the pressure itself.[16]

In this paper an approximate projection method related to the pressure correction approach is proposed to circumvent the above problem concerning the pressure computation. This is done by deriving the Poisson equation not for the pressure correction but for a related quantity. The homogeneous Neumann condition is still necessary for obtaining a divergence-free velocity (in the continuous sense at least), but since it now no longer holds for the pressure correction, it does not restrict the pressure computation. In the discrete sense, divergence freedom is only satisfied approximately, hence the classification *approximate* projection scheme.[17] It will also be shown that the solution of the projection scheme is consistent with that of the original Navier–Stokes equations. For the spatial discretization a high-order spectral element method[16,18] is chosen that exhibits excellent properties (small numerical diffusion and dispersion) for convection-dominated flows.

The outline of the paper is as follows. Section 2 presents the governing equations for incompressible fluid flow: the Navier–Stokes equations. In Section 3 the projection-decoupling scheme is presented. In order to discuss the theoretical background of the scheme, it is first applied to the Stokes equations. For the Navier–Stokes problem the equations are first split according to an operator-splitting procedure that decouples the treatment of convection and diffusion,[19] including the pressure term temporarily in the viscous part of the equations. This is discussed in Section 4. Next the velocity treatment is decoupled from the pressure treatment by applying the projection algorithm. The properties of the algorithm are extensively analysed by means of an analytical test case. In Section 5 more numerical results are presented for the problem of the flow over a backward-facing step. Finally, in Section 6, conclusions are drawn.

2. GOVERNING EQUATIONS

In this section, two-dimensional incompressible transient Newtonian flow is considered without thermal effects. Consider an open and bounded domain $\Omega \subset \mathbb{R}^d$ with boundary Γ for $t \geqslant 0$. The Navier–Stokes equations are given by the momentum equation

$$\frac{\partial \mathbf{u}}{\partial t} + (\mathbf{u} \cdot \nabla)\mathbf{u} - \nu \nabla^2 \mathbf{u} + \nabla p = \mathbf{f} \quad \text{in } \Omega \tag{1}$$

and the continuity equation, which implies that the flow is incompressible always and everywhere,

$$\nabla \cdot \mathbf{u} = 0 \quad \text{in } \bar{\Omega} \tag{2}$$

In these equations, $\mathbf{u}(\mathbf{x}, t) = (u_1, u_2)^T$ is the velocity vector, $p(\mathbf{x}, t)$ is the kinematic pressure, $\mathbf{f}(\mathbf{x}, t)$ is the body force vector and ν is the kinematic viscosity, which is assumed to be constant.

In order for the problem to be well-posed, boundary and initial conditions have to be imposed. With respect to boundary conditions it is necessary to prescribe either velocity (essential boundary conditions) or surface traction force (natural boundary conditions) in the normal and tangential directions.[3,13] Suppose for convenience that the boundary Γ is composed of two non-overlapping parts Γ_u and Γ_σ and assume that on each part either the velocity or the stress is prescribed. The boundary conditions can then be formulated as

$$\mathbf{u} = \mathbf{g}, \ \mathbf{x} \text{ on } \Gamma_u, \quad t \geqslant 0, \tag{3}$$

$$-p + \nu \frac{\partial u_n}{\partial n} = h_n \quad \text{and} \quad \nu\left(\frac{\partial u_n}{\partial \tau} + \frac{\partial u_\tau}{\partial n}\right) = h_\tau, \quad \mathbf{x} \text{ on } \Gamma_\sigma, \ t \geqslant 0, \tag{4}$$

with h_n, u_n the normal components and h_τ, u_τ the tangential components of the stress and the velocity respectively.

In an incompressible flow the pressure is an implicit variable whose value is (pointwise) determined by the requirement that the incompressibility constraint $\nabla \cdot \mathbf{u} = 0$ is satisfied there. The pressure can be prescribed in an indirect way via boundary condition (4). If, however, u_n is specified on all of Γ, thus prohibiting the boundary condition (4), the pressure is only obtainable up to an arbitrary additive constant. In that case one can further require that

$$\int_\Omega p \, d\Omega = 0. \tag{5}$$

Then also global mass conservation must be imposed through the boundary conditions, leading to the constraint

$$\int_\Gamma \mathbf{n} \cdot \mathbf{g} \, d\Gamma = 0. \tag{6}$$

Finally, initial conditions have to be imposed on the system. These read

$$\mathbf{u}(\mathbf{x}, 0) = \mathbf{u}_0, \quad \mathbf{x} \text{ in } \bar{\Omega}, \tag{7}$$

where $\mathbf{u}_0$ must satisfy

$$\nabla \cdot \mathbf{u}_0 = 0, \quad \mathbf{x} \text{ in } \bar{\Omega}, \tag{8}$$

$$\mathbf{n} \cdot \mathbf{u}_0 = \mathbf{n} \cdot \mathbf{g}(\mathbf{x}, 0), \quad \mathbf{x} \text{ on } \Gamma_u. \tag{9}$$

If either (8) or (9) is omitted, the problem (1), (2) is ill-posed.[3]

3. SOLUTION OF THE STOKES EQUATIONS

3.1. The projection scheme

In this subsection the properties of the projection method are analysed by means of its application to the linear Stokes problem. The solution algorithm can be applied to either the continuous or the discrete system of equations. In the latter case the procedure does not involve a rediscretization of the original equations. Consequently, the boundary conditions are then already built in directly in the weak or variational formulation, thereby prohibiting the need to formulate a specific boundary condition for the discrete 'Poisson' equation. In this case the choice of the element for the velocity and the pressure is important with respect to the well-posedness of the system. As is well-known from the theory of saddle-point problems, a discrete form of the Brezzi–Babuška condition[20] must then be satisfied for obtaining a unique velocity and pressure. For a high-order spectral element approximation this means that the degree of approximation for the pressure must be taken two degrees lower than that for the velocity.[21]

On the other hand, applying the decoupling procedure to the continuous equations leads to a more straightforward scheme, since in that case the original problem is reformulated into several new (and simpler) problems. The theory of saddle-point problems is then no longer applicable; as a consequence, the degree of approximation for velocity and pressure can be taken the same, yielding a simpler-to-implement numerical scheme. Moreover, then also iterative techniques suited for high-order systems, such as finite element preconditioning,[22,23] can easily be applied to the resulting discrete equations. In that case, however, the resulting Poisson equation requires a boundary condition. It will be shown that in the continuous projection scheme presented below, the use of a homogeneous Neumann boundary condition for the Poisson equation is valid and even essential in obtaining a divergence-free velocity field, while still the correct pressure can be obtained.

Consider the unsteady Stokes equations with, for simplicity, only essential boundary conditions:

$$\begin{aligned} &\frac{\partial \mathbf{u}}{\partial t} - \nu \nabla^2 \mathbf{u} + \nabla p = \mathbf{f} \quad \text{in} \quad \Omega, \\ &\nabla \cdot \mathbf{u} = 0 \quad \text{in} \quad \bar{\Omega}, \\ &\mathbf{u} = \mathbf{g} \quad \text{on} \quad \Gamma, \\ &\mathbf{u}(\mathbf{x}, 0) = \mathbf{u}_0 \quad \text{in} \quad \bar{\Omega}. \end{aligned} \tag{10}$$

The momentum equation can be written in the form

$$\frac{\partial \mathbf{u}}{\partial t} = \mathscr{D}\mathbf{u} - \nabla p + \mathbf{f}, \tag{11}$$

with $\mathscr{D} = \nu \nabla^2$ the diffusion operator. Equation (11) is integrated using an implicit backward difference scheme[24] with time step Δt. This yields the semidiscrete system

$$\frac{\beta_0 \mathbf{u}^{n+1} - \sum_{i=1}^{k} \beta_i \mathbf{u}^{n+1-i}}{\Delta t} = \mathscr{D}\mathbf{u}^{n+1} - \nabla p^{n+1} + \mathbf{f}^{n+1}. \tag{12}$$

The approximation of a quantity at time $t^{n+1} = (n+1)\Delta t$ is denoted by the superscript $n+1$. For a second-order backward difference scheme the following semidiscrete system results:

$$\begin{aligned} &\tfrac{3}{2}\mathbf{u}^{n+1} - \Delta t \mathscr{D}\mathbf{u}^{n+1} = 2\mathbf{u}^n - \tfrac{1}{2}\mathbf{u}^{n-1} - \Delta t \nabla p^{n+1} + \Delta t \mathbf{f}^{n+1} \quad \text{in } \Omega \\ &\nabla \cdot \mathbf{u}^{n+1} = 0 \quad \text{in } \bar{\Omega}, \\ &\mathbf{u}^{n+1} = \mathbf{g}^{n+1} \quad \text{on } \Gamma. \end{aligned} \tag{13}$$

The pressure correction scheme proposed in this study consists of a predictor–corrector procedure between the velocity and pressure fields and proceeds as follows.

1. Choose an appropriate predictor for the pressure,

$$p_{\mathrm{p}}^{n+1} = p_{\mathrm{p}}^{n+1}(p^n, p^{n-1}, \ldots), \tag{14}$$

such that at least $p_{\mathrm{p}}^{n+1} = p^{n+1} + \mathcal{O}(\Delta t)$.

In the present scheme the pressure at the previous time level is used for that purpose ($p_{\mathrm{p}}^{n+1} = p^n$), but also higher-order extrapolation can be used.

2. Compute a predictor for the velocity field ($\mathbf{u}_{\mathrm{p}}^{n+1}$) with the aid of the momentum equation and the predictor for the pressure:

$$\begin{aligned} &\tfrac{3}{2}\mathbf{u}_{\mathrm{p}}^{n+1} - \Delta t \mathscr{D}\mathbf{u}_{\mathrm{p}}^{n+1} = 2\mathbf{u}^n - \tfrac{1}{2}\mathbf{u}^{n-1} - \Delta t \nabla p_{\mathrm{p}}^{n+1} + \Delta t \mathbf{f}^{n+1} \quad \text{in } \boldsymbol{\Omega}, \\ &\mathbf{u}_{\mathrm{p}}^{n+1} = \mathbf{g}^{n+1} \quad \text{on } \boldsymbol{\Gamma}. \end{aligned} \tag{15}$$

As in this equation the pressure is treated explicitly, the incompressibility constraint has to be dropped and as a consequence the predicted velocity field $\mathbf{u}_{\mathrm{p}}^{n+1}$ in general will not be divergence-free. The choice of the boundary condition $\mathbf{u}_{\mathrm{p}}^{n+1} = \mathbf{g}^{n+1}$ implies that a pressure predictor that equals the exact pressure ($p_{\mathrm{p}}^{n+1} = p^{n+1}$) will result in a prediction of the velocity that equals the exact velocity ($\mathbf{u}_{\mathrm{p}}^{n+1} = \mathbf{u}^{n+1}$). Moreover, it will be shown below that for non-exact pressure predictors ($p_{\mathrm{p}}^{n+1} \neq p^{n+1}$) this choice results in a convenient boundary condition for the equations that determine the pressure corrector.

Correctors for the pressure (p_{c}^{n+1}) and velocity ($\mathbf{u}_{\mathrm{c}}^{n+1}$) will be formulated such that they satisfy the original momentum and continuity conditions in the internal region of the domain $\boldsymbol{\Omega}$:

$$\begin{aligned} &\tfrac{3}{2}\mathbf{u}_{\mathrm{c}}^{n+1} - \Delta t \mathscr{D}\mathbf{u}_{\mathrm{c}}^{n+1} = 2\mathbf{u}^n - \tfrac{1}{2}\mathbf{u}^{n-1} - \Delta t \nabla p_{\mathrm{c}}^{n+1} + \Delta t \mathbf{f}^{n+1} \quad \text{in } \boldsymbol{\Omega}, \\ &\nabla \cdot \mathbf{u}_{\mathrm{c}}^{n+1} = 0 \quad \text{in } \boldsymbol{\Omega}. \end{aligned} \tag{16}$$

Expressions for the velocity and pressure correctors can be obtained by subtracting the first equation of (16) from the first equation of (15). This yields

$$\tfrac{3}{2}(\mathbf{u}_{\mathrm{p}}^{n+1} - \mathbf{u}_{\mathrm{c}}^{n+1}) - \Delta t \mathscr{D}(\mathbf{u}_{\mathrm{p}}^{n+1} - \mathbf{u}_{\mathrm{c}}^{n+1}) = \Delta t \nabla (p_{\mathrm{c}}^{n+1} - p_{\mathrm{p}}^{n+1}) \quad \text{in} \quad \boldsymbol{\Omega}. \tag{17}$$

Taking the divergence of both parts of equation (17) and imposing the incompressibility constraint on $\nabla \cdot \mathbf{u}_{\mathrm{c}}^{n+1} = 0$ yields a Poisson equation of the form

$$\nabla^2 (p_{\mathrm{c}}^{n+1} - p_{\mathrm{p}}^{n+1} + \nu \nabla \cdot \mathbf{u}_{\mathrm{p}}^{n+1}) = \frac{3}{2\Delta t} \nabla \cdot \mathbf{u}_{\mathrm{p}}^{n+1} \quad \text{in} \quad \boldsymbol{\Omega}. \tag{18}$$

Here the vector identities $\nabla^2 \mathbf{v} = \nabla(\nabla \cdot \mathbf{v}) - \nabla \times (\nabla \times \mathbf{v})$ and $\nabla \cdot (\nabla \times \mathbf{v}) = 0$ are used, showing that the divergence and Laplace operators commute.

A unique solution of q^{n+1}, defined as

$$q^{n+1} = p_{\mathrm{c}}^{n+1} - p_{\mathrm{p}}^{n+1} + \nu \nabla \cdot \mathbf{u}_{\mathrm{p}}^{n+1}, \tag{19}$$

can only be obtained if equation (18) is equipped with a proper boundary condition. A boundary condition that is consistent with global mass conservation can be found if equation (18) is integrated over $\boldsymbol{\Omega}$ to give

$$\int_{\boldsymbol{\Omega}} \nabla^2 q^{n+1} \mathrm{d}\boldsymbol{\Omega} = \frac{3}{2\Delta t} \int_{\boldsymbol{\Omega}} \nabla \cdot \mathbf{u}_{\mathrm{p}}^{n+1} \mathrm{d}\boldsymbol{\Omega} \tag{20}$$

or equivalently

$$\int_\Gamma \frac{\partial q^{n+1}}{\partial n} d\Gamma = \frac{3}{2\Delta t} \int_\Gamma \mathbf{u}_p^{n+1} \cdot \mathbf{n} \, d\Gamma = 0. \tag{21}$$

This suggests a consistent choice of a homogeneous Neumann boundary condition for q^{n+1}:

$$\frac{\partial q^{n+1}}{\partial n} = 0 \quad \text{on } \Gamma. \tag{22}$$

3. Combining (18), (19) and (22), the following Poisson equation holds for q^{n+1}:

$$\begin{aligned} \nabla^2 q^{n+1} &= \frac{3}{2\Delta t} \nabla \cdot \mathbf{u}_p^{n+1} \quad \text{in } \Omega, \\ \frac{\partial q^{n+1}}{\partial n} &= 0 \quad \text{on } \Gamma. \end{aligned} \tag{23}$$

4. As q^{n+1} is a solution of a Poisson equation with a Neumann boundary condition, the corrected pressure at the time level $n+1$ can be computed from equation (19) as

$$p_c^{n+1} = q^{n+1} + p_p^{n+1} - \nu \nabla \cdot \mathbf{u}_p^{n+1} \tag{24}$$

up to an arbitrary constant.

5. The corrector $(\mathbf{u}_c^{n+1})$ is assumed to be of the form $\mathbf{u}_c^{n+1} = \mathbf{u}_p^{n+1} + \tilde{\mathbf{u}}$ such that $\nabla \cdot \mathbf{u}_c^{n+1} = \nabla \cdot \mathbf{u}_p^{n+1} + \nabla \cdot \tilde{\mathbf{u}} = 0$ in Ω. Equation (18) suggests that

$$\mathbf{u}_c^{n+1} = \mathbf{u}_p^{n+1} - \tfrac{2}{3} \Delta t \nabla q^{n+1} \tag{25}$$

is a good candidate.

Equation (25) does guarantee that $\mathbf{u}_c^{n+1} \cdot \mathbf{n} = \mathbf{g}^{n+1} \cdot \mathbf{n}$ on Γ by virtue of the homogeneous Neumann condition for q^{n+1} but does not guarantee that $\nabla \cdot \mathbf{u}_c^{n+1} = 0$ on Γ.

Some remarks

1. Substitution of the corrector velocity $\mathbf{u}_c^{n+1}$ and corrector pressure p_c^{n+1} as derived above into the first of equations (13) (using also equations (15) and (23) and supposing that the Laplacian and gradient commute) yields that this pair indeed satisfies the original momentum equations (13). The combination of (23) and (25) ensures that the corrector velocity satisfies divergence freedom in Ω. The boundary condition (22) ensures that the boundary conditions in the normal direction is satisfied. However, satisfaction of the boundary conditions in tangential directions is not ensured (see also the next couple of remarks). Consequently, divergence freedom of the corrector velocity on the boundary Γ is not proven.
2. Owing to the assumption that $p_p^{n+1} = p^{n+1} + \mathcal{O}(\Delta t)$, one may expect from (15) that also $\mathbf{u}_p^{n+1} = \mathbf{u}^{n+1} + \mathcal{O}(\Delta t)$ and thereby that $\nabla \cdot \mathbf{u}_p^{n+1} = \mathcal{O}(\Delta t)$. In that case equation (23) suggests that ∇q^{n+1} is bounded. Consequently, one may expect that (25) also ensures a consistent treatment of the boundary conditions in tangential directions.
3. All the available numerical results obtained with the present technique (particularly the results presented in this paper) advocate that the boundary conditions in tangential directions are also satisfied with second-order accuracy in time. This estimation, however, as well as the heuristic derivation given above, requires a more extensive analysis of the scheme, which is beyond the scope of this paper.

4. A way to impose the exact no-slip boundary condition for $\mathbf{u}_c^{n+1}$ could be to solve the momentum equation of system (16) (instead of using equation (25)) with p_c^{n+1} obtained from (24). Then, however, the incompressibility imposed by equation (25) will be lost. In that case it can be shown, under certain conditions of smoothness, that $L^{n+1} \equiv \nabla \cdot \mathbf{u}_c^{n+1}$ satisfies the Helmholtz equation

$$\frac{3}{2}\frac{L^{n+1}}{\Delta t} = \nu \nabla^2 L^{n+1}, \tag{26}$$

which has the solution $L^{n+1} \equiv 0$ if $L^{n+1} = 0$ or $\partial L^{n+1}/\partial n = 0$ on Γ. Since this cannot be ensured, $\nabla \cdot \mathbf{u}_c^{n+1}$ decays exponentially beyond a boundary layer of thickness $(\nu \Delta t)^{1/2}$, as is also pointed out by Orszag *et al.*,[12] which poses a severe restriction on the time step. Moreover, the final velocity field is not guaranteed to be divergence-free. Numerical experiments have indeed shown that with the above procedure $\nabla \cdot \mathbf{u}_c^{n+1}$ is worse compared with the results obtained with the projection scheme and that the maximum is achieved in the boundary layer. Thus with respect to divergence freedom the present algorithm is better suited.

5. Finally, with respect to initial conditions the initial velocity is given by equation (7); for the projection scheme also an initial condition for the pressure is required. The commonest way to obtain the initial pressure is to solve the pressure Poisson equation (PPE) with the Neumann boundary condition obtained from the momentum equation at $t = 0$.

3.2. *Spectral element discretization*

Application of a Galerkin spectral element discretization to the semidiscrete projection equations is performed in the standard way. As already stated in the previous subsection, there is no need to satisfy any form of the discrete Brezzi–Babuška condition, since the decoupling procedure is applied to the continuous equations, leading to uncoupled problems for both velocity and pressure. Therefore the degree of approximation for the pressure can be taken equal to that for the velocity, resulting in a numerical algorithm that is simple to implement. The fully discrete form of the projection scheme thus becomes as follows.

1. Calculate $\mathbf{u}_p^{n+1}$ by solving

$$\left(\tfrac{3}{2}\mathbf{M} + \Delta t \mathbf{D}\right)\mathbf{u}_p^{n+1} = 2\mathbf{M}\mathbf{u}^n - \tfrac{1}{2}\mathbf{M}\mathbf{u}^{n-1} - \Delta t \mathbf{Q}\mathbf{p}^n + \Delta t \mathbf{M}\mathbf{f}^{n+1}, \tag{27}$$

with $\mathbf{M}$ the (diagonal) mass matrix, $\mathbf{D}$ the diffusion matrix and $\mathbf{Q}$ the gradient matrix. The column $\mathbf{p}^n$ contains the pressure components at $t = t^n$. The column $\mathbf{f}$ contains also the contribution of non-homogeneous boundary conditions.

2. Calculate $\mathbf{q}^{n+1}$ by solving

$$\mathbf{K}\mathbf{q}^{n+1} = -\frac{3}{2\Delta t}\mathbf{L}\mathbf{u}_p^{n+1}, \tag{28}$$

with $\mathbf{K}$ the Laplacian matrix and $\mathbf{L}$ the divergence matrix.

3. Calculate $\mathbf{u}^{n+1}$ via

$$\mathbf{u}^{n+1} = \mathbf{u}_p^{n+1} - \tfrac{2}{3}\Delta t \mathbf{M}^{-1}\mathbf{Q}\mathbf{q}^{n+1}. \tag{29}$$

4. Calculate p^{n+1} via

$$\mathbf{p}^{n+1} = \mathbf{p}^n + \mathbf{q}^{n+1} - \nu \mathbf{M}^{-1}\mathbf{L}\mathbf{u}_p^{n+1}. \tag{30}$$

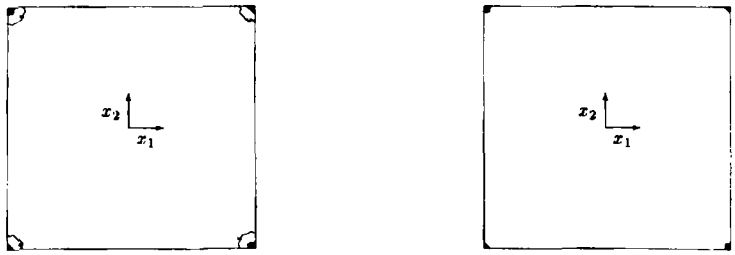

Figure 1. Contour plot of the pressure error for the Stokes problem with the projection method, using eight time steps (left) and 32 time steps (right)

From the above system it can be seen that it is essential that the mass matrix **M** is diagonal, since then the equations (29) and (30) do not involve the solution of a system, but only the calculation of matrix–vector products which can be performed at the elemental level. For high-order methods the use of a diagonal mass matrix is a valid approach with respect to accuracy, as is shown numerically by Timmermans and van de Vosse.[25]

Note that after spatial discretization, divergence freedom of the final computed velocity is only satisfied approximately, because from equations (28) and (29) it follows that

$$\mathbf{L}\mathbf{u}^{n+1} = \mathbf{L}\mathbf{u}_{\mathrm{p}}^{n+1} - \tfrac{2}{3}\Delta t\mathbf{L}\mathbf{M}^{-1}\mathbf{Q}\mathbf{q}^{n+1} = (\mathbf{I} + \mathbf{L}\mathbf{M}^{-1}\mathbf{Q}\mathbf{K}^{-1})\mathbf{L}\mathbf{u}_{\mathrm{p}}^{n+1} \neq 0, \tag{31}$$

since $\mathbf{K} \neq \mathbf{L}\mathbf{M}^{-1}\mathbf{Q}$. Also, the use of the diagonal mass matrix can further decrease the accuracy with which the incompressibility constraint is satisfied. However, the numerical results further on in this paper suggest that for a high-order method this loss of accuracy is not severe.

3.3. Application to an analytical test case

In order to test the performance of the projection scheme presented in the previous subsections, here a Stokes problem with an analytical solution is analysed. This analytical problem is adapted from Reference 26.

Consider the Stokes problem (10) with $\nu = 1$. The source term is chosen such that the exact velocity and pressure are given by

$$\begin{aligned} u_1(\mathbf{x}, t) &= -\cos(x_1)\sin(x_2)\mathrm{e}^{-2t}, \\ u_2(\mathbf{x}, t) &= \sin(x_1)\cos(x_2)\mathrm{e}^{-2t}, \\ p(\mathbf{x}, t) &= -\tfrac{1}{4}[\cos(2x_1) + \cos(2x_2)]\mathrm{e}^{-4t}. \end{aligned} \tag{32}$$

The problem is solved on the domain $\Omega = (-1, 1) \times (-1, 1)$ with time-dependent boundary conditions for the velocity according to equation (32) and with initial velocity and pressure according to equation (32) at $t = 0$. The domain Ω is divided into $n_{\mathrm{e}} = 4$ elements of degree n. As a first test, this problem is approximated until $t = 1$ using a degree of approximation n such that the spatial errors are negligible compared with the errors due to the time integration.

In Table I results are presented for a varying number of time steps for the velocity and its discrete divergence, and for the pressure and its discrete gradient, for the projection scheme. The scheme is second-order in time for the velocity and for the gradient of the pressure. The results are especially accurate with respect to divergence freedom. The results for the pressure itself are really bad, realizing that the maximum value of the pressure at $t = 1$ is $\mathcal{O}(10^{-2})$. Since it is shown that the pressure satisfies the PPE with the correct Neumann condition and is therefore consistent with the original Stokes equation, this may seem surprising. The picture becomes clearer if it is known where the error in the

Table I. Stokes problem with analytical solution. Predictor–corrector method. Discrete maximum error ε for several quantities; spatial discretization fixed, number of time steps varying

Time steps	Discrete maximum error			
	u	**Lu**	**p**	**Qp**
8	$0{\cdot}47 \times 10^{-3}$	$0{\cdot}82 \times 10^{-5}$	$0{\cdot}27 \times 10^{0}$	$0{\cdot}17 \times 10^{-2}$
16	$0{\cdot}10 \times 10^{-3}$	$0{\cdot}12 \times 10^{-5}$	$0{\cdot}19 \times 10^{0}$	$0{\cdot}27 \times 10^{-3}$
32	$0{\cdot}24 \times 10^{-4}$	$0{\cdot}19 \times 10^{-6}$	$0{\cdot}18 \times 10^{0}$	$0{\cdot}50 \times 10^{-4}$
64	$0{\cdot}58 \times 10^{-5}$	$0{\cdot}47 \times 10^{-7}$	$0{\cdot}10 \times 10^{0}$	$0{\cdot}13 \times 10^{-4}$

Table II. Stokes problem with analytical solution. Predictor–corrector method with Dirichlet boundary conditions for the pressure. Discrete maximum error ε for several quantities; spatial discretization fixed, number of time steps varying

Time steps	Discrete maximum error			
	u	**Lu**	**p**	**Qp**
8	$0{\cdot}14 \times 10^{-2}$	$0{\cdot}23 \times 10^{-3}$	$0{\cdot}34 \times 10^{-3}$	$0{\cdot}40 \times 10^{-4}$
16	$0{\cdot}64 \times 10^{-3}$	$0{\cdot}77 \times 10^{-4}$	$0{\cdot}13 \times 10^{-3}$	$0{\cdot}56 \times 10^{-5}$
32	$0{\cdot}99 \times 10^{-4}$	$0{\cdot}11 \times 10^{-4}$	$0{\cdot}70 \times 10^{-5}$	$0{\cdot}47 \times 10^{-6}$
64	$0{\cdot}14 \times 10^{-4}$	$0{\cdot}13 \times 10^{-5}$	$0{\cdot}33 \times 10^{-5}$	$0{\cdot}14 \times 10^{-6}$

pressure achieves its maximum value. In Figure 1 a contour plot of the pressure error is given for several time steps. The maximum error is clearly obtained near the corner points. The reason why the computed pressure is not correct is because for this test case the boundary is not smooth owing to the corners. The use of a Neumann condition overdetermines the problem at the corner points.

It is proven by Gresho and Sani[13] that for a sufficiently smooth boundary the pressure obtained from the PPE with the Neumann condition will also satisfy the Dirichlet boundary condition which follows from the tangential component of the momentum equation. If the Dirichlet boundary condition is used, the Poisson problem for the pressure is well-posed and should yield the correct pressure. To emphasize this point, the same computations are made with the correct Dirichlet boundary conditions for the Poisson equation. Table II gives the results for the projection scheme. The pressure now is clearly correct. Moreover, the pressure gradient has improved considerably. It can also be seen that since the zero Neumann boundary condition no longer holds now, the velocity and its divergence freedom have deteriorated compared with the results in Table I.

In the second test the problem is approximated until $t = 0{\cdot}5$ using $n_e = 4$ elements with varying degree of freedom n, but now trying to keep the time step small enough to preclude temporal errors. The results for the projection scheme are presented in Figure 2 (left). Spectral convergence is obtained for the velocity and for the discrete gradient of the pressure (note that from $N = 13$ onwards the time step is not yet small enough to preclude errors due to time integration). The pressure itself is not correct. Again performing the same computation, but now with the correct Dirichlet boundary conditions for the pressure, also gives spectral convergence for the pressure as shown in Figure 2 (right).

4. SOLUTION OF THE NAVIER–STOKES EQUATIONS

4.1. The operator-splitting approach

Consider again the Navier–Stokes equations plus boundary and initial conditions formulated in Section 2. The first step in the solution method is to apply a similar operator-splitting technique to that

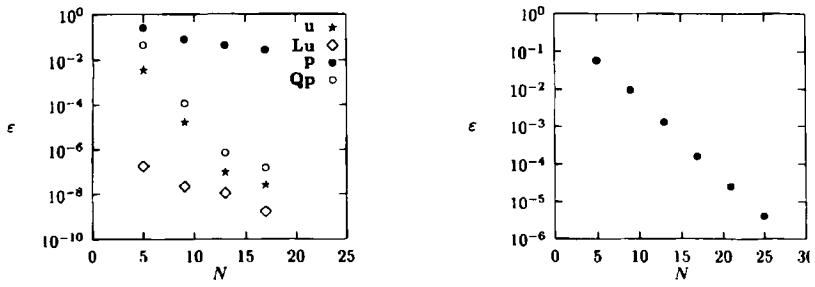

Figure 2. Stokes problem. Evolution of the discrete maximum error ε for several quantities (left) and for the pressure in the case of Dirichlet conditions (right) with $n_c = 4$, n varying. N is the number of degrees of freedom in one direction

described in Reference 8 for unsteady convection–diffusion problems, including the pressure term temporarily in the viscous part of the equation. The momentum equation is written in the form

$$\frac{\partial \mathbf{u}}{\partial t} = \mathscr{D}\mathbf{u} + \mathscr{C}\mathbf{u} - \nabla p + \mathbf{f}, \tag{33}$$

with $\mathscr{D} = (\nu\nabla^2)$ the diffusion operator and $\mathscr{C} = -(\mathbf{u}\cdot\nabla)$ the non-linear convection operator. Equation (33) is written in terms of an integrating factor in $\mathscr{C}$:[19]

$$\frac{\partial}{\partial t}\left(\mathscr{Q}_{\mathscr{C}}^{(t^*,t)}\mathbf{u}\right) = \mathscr{Q}_{\mathscr{C}}^{(t^*,t)}(\mathscr{D}\mathbf{u} - \nabla p + \mathbf{f}). \tag{34}$$

The 'Stokes' equation (34) is integrated using an implicit backward difference scheme with time step Δt. This yields the semidiscrete system

$$\frac{\beta_0\mathbf{u}^{n+1} - \sum_{i=1}^{k}\beta_i\mathscr{Q}_{\mathscr{C}}^{(t^{n+1},t^{n+1-i})}\mathbf{u}^{n+1-i}}{\Delta t} = \mathscr{D}\mathbf{u}^{n+1} - \nabla p^{n+1} + \mathbf{f}^{n+1}. \tag{35}$$

To evaluate the terms $\mathscr{Q}_{\mathscr{C}}^{(t^{n+1},t^{n+1-i})}\mathbf{u}^{n+1-i}$ $(i = 1, 2, \ldots)$, the associated initial value problem

$$\begin{aligned} &\frac{\partial\tilde{\mathbf{u}}(s)}{\partial s} = \mathscr{C}\tilde{\mathbf{u}}(s), \quad 0 < s < i\Delta t, \\ &\tilde{\mathbf{u}}(0) = \mathbf{u}^{n+1-i} \end{aligned} \tag{36}$$

is solved, from which it follows that

$$\mathscr{Q}_{\mathscr{C}}^{(t^{n+1},t^{n+1-i})}\mathbf{u}^{n+1-i} = \tilde{\mathbf{u}}(i\Delta t). \tag{37}$$

Problem (36), accounting for the non-linear convection, is solved using a three-step explicit Taylor–Galerkin scheme also used by Jiang and Kawahara.[27] This scheme is, for linear systems, third-order-accurate in time. The initial condition is $\tilde{\mathbf{u}}^0 = \mathbf{u}^{n+1-i}$; a time step Δs such that $\Delta t = j\Delta s$ with j an integer is used. The semidiscrete convection step then becomes

$$\begin{aligned} \tilde{\mathbf{u}}^{m+1/3} &= \tilde{\mathbf{u}}^m - \frac{\Delta s}{3}(\tilde{\mathbf{u}}^m\cdot\nabla)\tilde{\mathbf{u}}^m, \\ \tilde{\mathbf{u}}^{m+1/2} &= \tilde{\mathbf{u}}^m - \frac{\Delta s}{2}(\tilde{\mathbf{u}}^{m+1/3}\cdot\nabla)\tilde{\mathbf{u}}^{m+1/3}, \\ \tilde{\mathbf{u}}^{m+1} &= \tilde{\mathbf{u}}^m - \Delta s(\tilde{\mathbf{u}}^{m+1/2}\cdot\nabla)\tilde{\mathbf{u}}^{m+1/2}. \end{aligned} \tag{38}$$

After introduction of the simpler notation $\tilde{\mathbf{u}}^{n+1-i} = \mathscr{Q}^{(t^{n+1-i},t^n)}\mathbf{u}^{n+1-i}$, equation (37) leads to

$$\tilde{\mathbf{u}}^{n+1-i} = \tilde{\mathbf{u}}^{i(j+1)}. \tag{39}$$

The further deduction of the projection scheme is completely analogous to the Stokes case; also, the theory concerning boundary conditions and consistency of the computed solution holds now. The only difference consists of the equation for the intermediate velocity.

For a second-order backward difference integration this part reads: calculate $\mathbf{u}_p^{n+1}$ from

$$\tfrac{3}{2}\mathbf{u}_p^{n+1} - \Delta t\mathscr{D}\mathbf{u}_p^{n+1} = 2\tilde{\mathbf{u}}^n - \tfrac{1}{2}\tilde{\mathbf{u}}^{n-1} - \Delta t\nabla p^n + \Delta t\mathbf{f}^{n+1}, \tag{40}$$

with $\mathbf{u}_p^{n+1} = \mathbf{g}^{n+1}$ on Γ. The quantities $\tilde{\mathbf{u}}^n$ and $\tilde{\mathbf{u}}^{n-1}$ are calculated according to the associated convection problem (38), (39).

The spectral element discretization of equation (40) is given by: calculate $\mathbf{u}_p^{n+1}$ by solving

$$\left(\tfrac{3}{2}\mathbf{M} + \Delta t\mathbf{D}\right)\mathbf{u}_p^{n+1} = 2\mathbf{M}\tilde{\mathbf{u}}^n - \tfrac{1}{2}\mathbf{M}\tilde{\mathbf{u}}^{n-1} - \Delta t\mathbf{Q}\mathbf{p}^n + \Delta t\mathbf{M}\mathbf{f}^{n+1}. \tag{41}$$

The columns $\tilde{\mathbf{u}}^n$ and $\tilde{\mathbf{u}}^{n-1}$ are calculated through the solution of

$$\begin{aligned}
\tilde{\mathbf{u}}^{m+1/3} &= \tilde{\mathbf{u}}^m - \frac{\Delta s}{3}\mathbf{M}^{-1}\mathbf{C}^m\tilde{\mathbf{u}}^m,\\
\tilde{\mathbf{u}}^{m+1/2} &= \tilde{\mathbf{u}}^m - \frac{\Delta s}{2}\mathbf{M}^{-1}\mathbf{C}^{m+1/3}\tilde{\mathbf{u}}^{m+1/3},\\
\tilde{\mathbf{u}}^{m+1} &= \tilde{\mathbf{u}}^m - \Delta s\mathbf{M}^{-1}\mathbf{C}^{m+1/2}\tilde{\mathbf{u}}^{m+1/2},
\end{aligned} \tag{42}$$

where $\mathbf{C}^{m+1/3}$ and $\mathbf{C}^{m+1/2}$ denote the convection matrices at time levels $m+\frac{1}{3}$ and $m+\frac{1}{2}$ respectively.

Again, the use of a diagonal mass matrix $\mathbf{M}$ ensures an efficient evaluation without the need to solve the system.

4.2. The analytical test case revisited

Consider again the analytical velocity and pressure given by equation (32). For $\nu = 1$ this solution satisfies the Navier–Stokes equations with zero source term. The numerical results for this test case are quite similar to those obtained for the Stokes problem, as can be expected. To emphasize that the projection scheme performs well also in the presence of a non-linear convective term, the second test of Section 3.3 is repeated. The problem is approximated until $t = 0{\cdot}5$ using $n_e = 4$ elements of varying degree of approximation n, keeping the time step small enough to ensure that temporal errors are negligible. Figure 3 (left) shows the results for the scheme using the imposed Neumann condition for the Poisson equation. Spectral accuracy is obtained for the velocity and the discrete gradient of the pressure. For the pressure itself, again spectral accuracy can be achieved using the correct Dirichlet boundary condition, as shown in Figure 3 (right).

5. FLOW OVER A BACKWARD-FACING STEP

As a second test case for the validation of the Navier–Stokes algorithm, the flow over a backward-facing step in a channel is considered. The computational domain and boundary conditions are shown in Figure 4. The geometry is taken to be the same as that used in Reference 26. The height of the step, the height of the channel and the length of the channel are taken to be $h = \frac{1}{2}$, $H = 1$ and $l = 15$ (30 step heights) respectively. At the inflow boundary, located at the step, a parabolic profile $u_1 = g(x_2) = 24x_2(\frac{1}{2} - x_2)$, $u_2 = 0$ is prescribed ($x_2 = 0$ is taken to be the horizontal midline of the channel). It is customary to prescribe zero stress at the outflow boundary: $h_n = h_\tau = 0$; see equation (4). In formulations where a pressure Poisson equation has to be solved to obtain the pressure (as is the case

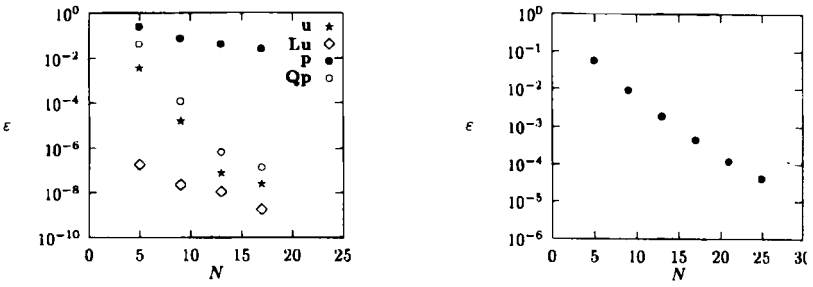

Figure 3. Navier–Stokes problem. Evolution of the discrete maximum error ε for several quantities (left) and for the pressure in the case of Dirichlet conditions (right) with $n_e = 4$, n varying. N is the number of degrees of freedom in one direction

with the present algorithm), the most frequently used outflow boundary condition for the pressure problem is $p = 0$ in combination with homogeneous Neumann conditions for the velocity components, since it results in no coupling between the pressure and velocity calculations. The Neumann conditions for the velocity are implemented naturally in the variational formulation; also, Neumann conditions for the velocity on the outflow perform better than Dirichlet conditions because they are less restrictive. Finally, on the walls of the channel, no-slip boundary conditions are assumed.

The flow at three different values of the Reynolds number, $Re = 100$, 200 and 400, is analysed. For these values of Re the flow is still laminar. The behaviour of the flow at higher values of Re, more specifically at $Re = 800$, is currently being investigated. In particular, since there is recent discussion in the literature about the stability of the flow for this value of Re when using high-order spatial discretization techniques,[28] a thorough and detailed analysis of the numerical results is required. The purpose of this paper is to validate the projection scheme by means of some test cases.

The computations are performed until the steady state is reached using a spectral element mesh of $n_e = 32$ elements (eight elements in the horizontal and four in the vertical direction) with degree of approximation $n = 8$. This leads to a total of 65×33 grid points, a much coarser mesh than that used by Kim and Moin.[26] A plot of the spectral element mesh is given in Figure 5. Streamlines of the resulting steady flow for the different values of Re are shown in Figure 6. An excellent test of the accuracy of the numerical scheme is to measure the value of the reattachment length r with respect to Re. In Table III the values of the reattachment length divided by the step height h are given for both the present computations and the computations performed by Kim and Moin.[26] It can be seen that they compare very well.

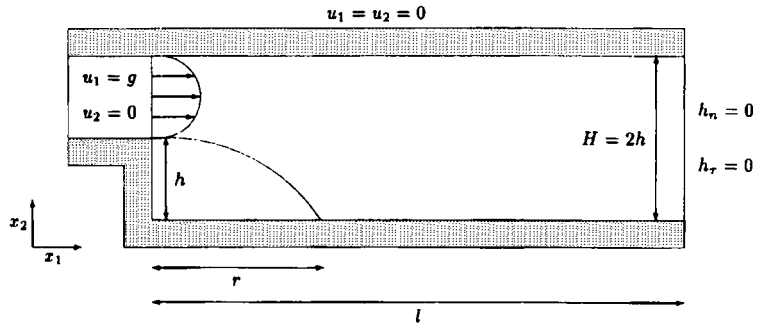

Figure 4. Flow over a backward-facing step. Computational domain and boundary conditions (1 : 4 domain aspect ratio)

Table III. Flow over a backward-facing step. Reattachment length r divided by step height h as a function of Reynolds number Re for the present computations and for the computations of Kim and Moin[26]

	r/h	
Re	Present	Kim and Moin
100	3·2	3·2
200	5·4	5·3
400	8·5	8·6

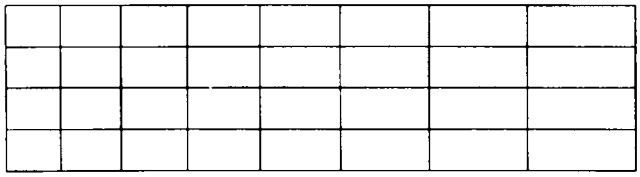

Figure 5. Flow over a backward-facing step. Spectral element mesh used (1 : 4 domain aspect ratio)

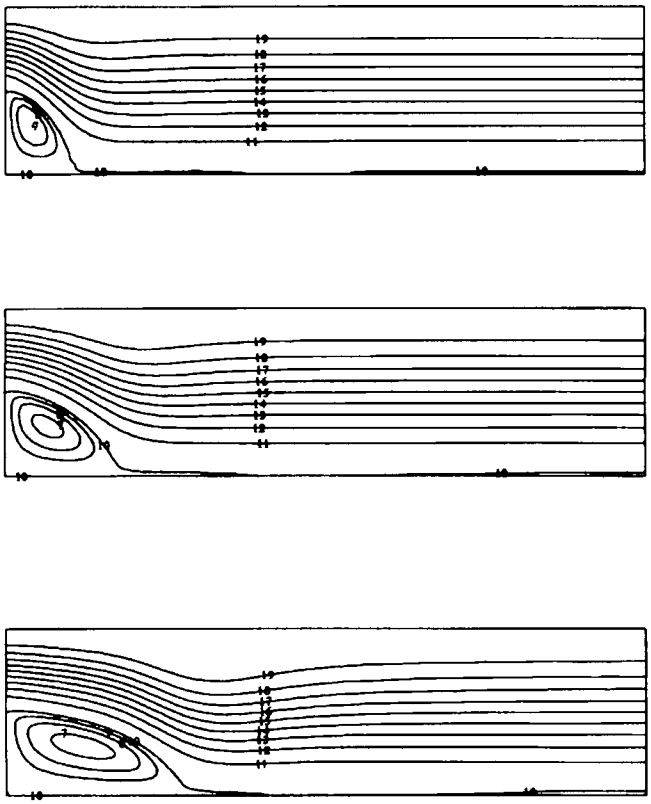

Figure 6. Flow over a backward-facing step (1 : 4 domain aspect ratio). Streamlines at $Re = 100$ (top), $Re = 200$ (centre) and $Re = 400$ (bottom) for $n_e = 8 \times 4$ elements of degree $n = 8$

6. CONCLUSIONS

This paper has dealt extensively with the solution of the Navier–Stokes equations for unsteady incompressible flow. The choice of solution method is largely determined by the need for an efficient numerical scheme. The solution method presented consists of a continuous projection scheme with second-order accuracy in time. The method can be classified as a special application of the class of projection methods. In a projection method the original set of Navier–Stokes equations is split into a set of problems that are simple to solve for both velocity and pressure. In the projection approach the velocity and pressure are decoupled by taking the pressure at the previous time level, resulting in a convection–diffusion problem for an intermediate velocity field that can be solved using an operator-splitting technique. Both velocity and pressure are then corrected. This results in a second-order-consistent algorithm.

Gresho and Sani[13] emphasize the following weak points of a 'projection' approach.

1. *More-than-originally necessary smoothness for velocity and pressure are required.*
2. *It is difficult to derive a boundary condition for the pressure, since it involves the calculation of second-order derivatives of the velocity.* In the present algorithm this problem does not exist. The boundary condition (a homogeneous Neumann condition) to be formulated is for a related quantity and not for the pressure itself.
3. *There is generally no discrete divergence-free condition that will be satisfied by the computed velocity field.* This is also true for the computed velocity of the fully discretized projection scheme, i.e. divergence freedom is only satisfied in the weak sense. However, in the continuous formulation the final velocity is guaranteed to be divergence-free, since the incompressibility constraint is applied to the new velocity at each time level and not to the intermediate velocity as is the case in the classical splitting approach.
4. *The solvability constraint for the pressure Poisson equation is often difficult to satisfy.* In the present case this constraint, formulated by

$$\int_{\Gamma} \mathbf{n} \cdot \mathbf{u}_{\mathrm{p}}^{n+1} \mathrm{d}\Gamma = 0, \tag{43}$$

is automatically satisfied because of the choice of boundary conditions for the intermediate velocity.

The algorithm has been thoroughly analysed by means of a test case with analytical velocity and pressure. Especially with respect to divergence freedom the scheme gives excellent results. Moreover, the scheme is clearly second-order-consistent in time for both the velocity and the gradient of the pressure. A 'practical' drawback for the computation of the pressure is a smoothness requirement for the boundary. For the test case the Poisson problem is overdetermined at the corner points because of the use of the (imposed) Neumann condition. If the correct Dirichlet boundary condition is used, the scheme yields the correct pressure. Therefore a way to compute the pressure in the case of a non-smooth boundary could be to retrieve it through postprocessing of the discrete gradient on the boundary, yielding an accurate approximation of the Dirichlet boundary condition. The scheme has been further validated by simulating the laminar flow over a backward-facing step. For this test case also, excellent results are obtained.

With respect to the spectral element discretization the above algorithm has several advantages. Firstly, the application of the decoupling algorithm to the continuous Navier–Stokes problem results in a set of equations that is simple to implement. The degree of approximation for velocity and pressure can be taken the same, as there is no need to satisfy any form of the Brezzi–Babuška condition. Secondly, the use of a diagonal mass matrix, which is a valid approach in a high-order method, is essential with respect

to efficiency, since in that case both the convective equations for velocity and the correction equations for velocity and pressure do not involve the solution of a system, but only the calculation of matrix–vector products which can be performed at the elemental level. Finally, for the analytical test case it was also shown that spectral accuracy for both velocity and pressure can be achieved if the temporal errors are negligible.

ACKNOWLEDGEMENTS

The authors would like to acknowledge support by the Dutch Foundation of Technology (STW), grant EWT 81.1442, and by the J. M. Burgers Centre for Fluid Mechanics.

REFERENCES

1. M. Fortin and R. Glowinski, *Augmented Lagrangian Methods: Applications to the Numerical Solution of Boundary Value Problems*, North-Holland, Amsterdam, 1983.
2. R. Peyret and T. D. Taylor, *Computational Methods for Fluid Flow*, Springer, New York, 1983.
3. R. Temam, *Navier–Stokes Equations*, North-Holland, Amsterdam, 1984.
4. V. Girault and P. A. Raviart, *Finite Element Methods for Navier–Stokes Equations*, Springer, New York, 1986.
5. P. M. Gresho, 'Some current CFD issues relevant to the incompressible Navier–Stokes equations', *Comput. Methods Appl. Mech. Eng.*, **87**, 201–252 (1991).
6. A. J. Chorin, 'Numerical solution of the Navier–Stokes equations', *Math. Comput.*, **22**, 745–761 (1968).
7. P. M. Gresho, 'On the theory of semi-implicit projection methods for viscous incompressible flow and its implementation via a finite element method that also introduces a nearly consistent mass matrix. Part 1: Theory', *Int. j. numer. methods fluids*, **11**, 587–620 (1990).
8. J. Shen, 'On error estimates of some higher order projection and penalty-projection methods for Navier–Stokes equations', *Numer. Math.*, **62**, 49–73 (1992).
9. G. E. Karniadakis, M. Israeli and S. A. Orszag, 'High-order splitting schemes for the incompressible Navier–Stokes equations', *J. Comput. Phys.*, **97**, 414–443 (1991).
10. J. Donea, S. Giulani, H. Laval and L. Quartapelle, 'Finite element solution of the unsteady Navier–Stokes equations by a fractional step method', *Comput. Methods Appl. Mech. Eng.*, **30**, 53–73 (1982).
11. H. Laval and L. Quartapelle, 'A fractional-step Taylor–Galerkin method for unsteady incompressible flows', *Int. j. numer. methods fluids*, **11**, 501–513 (1990).
12. S. A. Orszag, M. Israeli and M. O. Deville, 'Boundary conditions for incompressible flows', *J. Sci. Comput.*, **1**, 75–111 (1986).
13. P. M. Gresho and R. L. Sani, 'On pressure boundary conditions for the incompressible Navier–Stokes equations', *Int. j. numer. methods fluids*, **7**, 1111–1145 (1987).
14. J. van Kan, 'A second-order accurate pressure-correction scheme for viscous incompressible flows', *SIAM J. Sci. Stat. Comput.*, **7**, 870–891 (1986).
15. D. M. Hawken, H. R. Tamaddon-Jahromi, P. Townsend and M. F. Webster, 'A Taylor–Galerkin based algorithm for viscous incompressible flow', *Int. j. numer. methods fluids*, **10**, 327–351 (1990).
16. L. J. P. Timmermans, 'Analysis of spectral element methods with application to incompressible flow', *Ph.D. Thesis*, Eindhoven University of Technology, 1994.
17. P. M. Gresho, R. Sani and M. Engleman, *Incompressible Flow and the Finite Element Method*, Wiley, Chichester, 1996.
18. Y. Maday and A. T. Patera, 'Spectral element methods for the incompressible Navier–Stokes equations', in A. Noor (ed.), *State-of-the-Art Surveys on Computational Mechanics*, ASME, New York, 1989, pp. 71–143.
19. L. J. P. Timmermans, F. N. van de Vosse and P. D. Minev, 'Taylor–Galerkin based spectral element methods for convection–diffusion problems', *Int. j. numer. methods fluids*, **18**, 853–870 (1994).
20. F. Brezzi, 'On the existence, uniqueness and approximation of saddle-point problems arising from Lagrangian multipliers', *RAIRO*, **8**, 129–151 (1974).
21. Y. Maday, A. T. Patera and E. M. Rønquist, 'A well-posed optimal spectral element approximation for the Stokes problem', *ICASE Rep. 87-48*, NASA Langley Research Center, Hampton, VA, 1987.
22. M. Deville and E. Mund, 'Chebyshev pseudospectral solution of second order elliptic equations with finite element preconditioning', *J. Comput. Phys.*, **60**, 517–533 (1985).
23. L. J. P. Timmermans and F. N. van de Vosse, 'Finite element preconditioned spectral element methods for convection–diffusion problems', in J. F. Dijskman and F. T. M. Nieuwstadt (eds), *Topics in Applied Mechanics: Integration of Theory and Application in Applied Mechanics*, Kluwer, Dordrecht, 1993, pp. 363–370.
24. E. Hairer, G. Wanner and S. P. Noersett, *Solving Ordinary Differential Equations I. Nonstiff Problems*, Springer, Berlin, 1987.

25. L. J. P. Timmermans and F. N. van de Vosse, 'Spectral methods for advection–diffusion problems', in C. B. Vreugdenhil and B. Koren (eds), *Notes on Numerical Fluid Mechanics: Numerical Methods for Advection–Diffusion Problems*, Vieweg, Braunschweig, 1993, pp. 171–194.
26. J. Kim and P. Moin, 'Application of a fractional-step method to incompressible Navier–Stokes equations', *J. Comput. Phys.*, **59**, 308–323 (1985).
27. C. B. Jiang and M. Kawahara, 'A three-step finite element method for unsteady incompressible flows', *Comput. Mech.*, **11**, 355–370 (1993).
28. P. M. Gresho, D. K. Gartling, J. R. Torczynski, K. A. Cliffe, K. H. Winters, T. J. Garratt, A. Spence and J. W. Goodrich, 'Is the steady viscous incompressible two-dimensional flow over a backward-facing step at $Re = 800$ stable', *Int. j. numer. methods fluids*, **17**, 501–541 (1993).